Acquisition of Innate Odor Preference Depends on Spontaneous and Experiential Activities During Critical Period

Qiang Qiu[1], Yunming Wu[1], Limei Ma[1], Vivekanandan Ramalingam[1,3] and C. Ron Yu[1, 2,†]

[1]Stowers Institute for Medical Research, 1000 East 50th Street, Kansas City, MO 64110

[2]Department of Anatomy and Cell Biology, University of Kansas Medical Center, 3901 Rainbow Boulevard, Kansas City, KS 66160

[3]Interdisciplinary Graduate Program in Biomedical Sciences, University of Kansas Medical Center, 3901 Rainbow Boulevard, Kansas City, KS 66160

[†]Correspondence: 816-926-4334 (office)

cry@stowers.org

Abstract

Animals possess inborn ability to recognize certain odors, which enables them to seek food, avoid predators and find mates even in the absence of prior experiences. Here we report that the acquisition of innate odor recognition requires spontaneous neural activity and is influenced by sensory experience during early postnatal development. Genetic silencing of mouse olfactory sensory neurons during the critical period has little impact on odor sensitivity, odor discrimination and recognition later in life. However, it abolishes innate odor preference and alters the patterns of activation in brain centers associated with odor preference. Moreover, exposure to an innately aversive odor during the critical period abolishes aversion in adulthood in an odor specific manner. The loss of innate aversion is associated with broadened projection of OSNs expressing the cognate receptor such that they innervate ectopic glomeruli in the olfactory bulb. These results indicate that a delicate balance of neural activity is required during critical period in establishing innate odor preference and that ectopic projection is a convergent mechanism to alter innate odor valence.

Introduction

Behavioral characteristics are often described as either acquired or innate. While most environmental stimuli do not carry obvious ethological values, animals can develop characteristic responses through associative learning and assign valence to individual stimulus. During this process, the neural circuits underlying the behaviors must be modifiable by sensory experiences. However, animals can also react innately to some stimuli with instinctive responses that are thought to be pre-programmed in the neural circuits. These fixed action patterns likely have evolved to deal with stimuli in the animal's immediate environment that carry information about the inherent values of the signals. Odor-based predator avoidance, food seeking, pheromone-induced territorial aggression and mating are examples of such innate responses. The exhibition of stereotypical responses to these stimuli often has an onset associated with developmental stages and does not require any prior experience.

What is the basis of the neural circuits that mediate innate versus learned behaviors? All neural circuits are specified by genetic factors. However, whether sensory experience and neural activity influence the development of the connectivity is thought to distinguish the two types of behavioral responses. In most sensory systems, circuit modification by sensory experience underlies behavioral adaptation. In the mammalian brain, circuit connections are sensitive to sensory deprivation during early postnatal development in a time window defined as the critical period [1,2]. Learning further modifies circuit

connections to allow flexible assignment of valence to specific sensory stimuli. Circuit motifs such as divergent paths and opposing components allow adaptive changes that are thought to mediate these flexible assignments [3].

On the other hand, circuits that underlie innate responses are thought to be insensitive to sensory experiences. Innateness is defined by stereotypical responses to the stimuli without prior experience or associative learning, suggesting that neural circuits that process the inherent valence of stimuli are genetically hardwired to channel sensory information directly to motor or endocrine output. In other words, the neurons in the circuits form labeled lines that directly translate stimuli into actions. The labeled lines are thought to be insulated from influences of other sensory channels that transmit signals that broadly represent environmental stimuli. The formation of the innate circuits should not be influenced by sensory experience or subject to changes during development. This assumption has not been experimentally tested.

The olfactory system offers an ideal system to study both leaned and innate responses to sensory stimuli. A repertoire of ~1000 functional odorant receptors, 15 TAARs, and a family of MS4 receptors detect volatile odors [4-7]. Olfactory sensory neurons expressing the same odorant receptor converge their axons into a few glomeruli stereotypically positioned in the olfactory bulb forming a topographic map [8]. This convergent glomerular map is thought to be essential for encoding odor quality. Odors activate disparate sets of glomeruli and the patterns are transformed by the mitral/tufted cells in the olfactory bulb

before the information is passed to the olfactory cortices. The patterns of activity in the cortical areas can be learned through association with other stimuli. Mice are also intrinsically attracted by food odors and conspecific urine but avoid odors from decomposing flesh or predators. The dorsal area of the olfactory bulb is shown to be required for innate responses to aversive odors; other studies have shown that a few odorant receptors are both sufficient and necessary to trigger innate responses to specific odors [9-13].

During development, OSNs firing spontaneous action potentials that are shown to originate from ligand-independent activity of the odorant receptors [14,15]. The receptor activities drive specific temporal patterns of action potential firing [16]. Spontaneous activity influences the development of the olfactory glomerular map during the critical period [17-19]. The olfactory map that formed during the critical period is imprinted into adulthood. However, it has not been clear whether changes caused by levels of spontaneous activity have any impact on odor detection, learned and innate odor discrimination and recognition. In this study, we address how spontaneous activities and odor experience during early postnatal period influence odor-guided behaviors in adulthood.

Results

Spontaneous neural activity during early development is not required for odor detection

In previous studies, we have developed a genetic approach to silence the spontaneous activity during development [15,18] (Fig. 1a-i). Silencing the OSNs during the critical period led to coarsened projection patterns of olfactory axons [18,19]. Using the *OMP-IRES-tTA / tetO-Kir2.1-IRES-taulacZ* compound heterozygotic mice [15], we were able to restrict the expression of Kir2.1 channel to the pre-weaning period (Fig. 1a-ii). Feeding the *Kir2.1* mice with doxycycline (DOX) after postnatal day 21 (P21) suppressed *Kir2.1* expression [18]. In these DOX-treated mice (referred to as the Kir2.1-off mice), we used cell-attached patch clamp to record spontaneous activity from the dendritic knobs of sensory neurons expressing the *M72* OR gene [20] (Fig. 1b-i). Neurons in Kir2.1-off mice displayed similar inter spike interval and spontaneous firing rate compared to those in the control mice (Fig. 1b-ii-iv). In electro-olfactogram (EOG) recordings, which measured the field potential of odor-evoked responses, we found that there was no discernible difference in the amplitude and time course of odor-evoked responses between control and Kir2.1-off mice (Fig. 1c). Thus, DOX treatment restored neural activity in the OSNs of Kir2.1-off animals.

We used the Kir2.1-off mice to test whether neuronal silencing altered the ability of the mice to detect, discriminate and recognize odors. We first evaluated detection of low concentration of amyl acetate (AA) and 2-heptanone (HPO) using a dishabituation assay that provided a sensitive readout of odor detection threshold in naïve animals [21]. Control and Kir2.1-off mice exhibited similar increase in investigation of the odor port with increasing concentration of odors (Fig. 1d-i and Supplementary Fig. 1a). The thresholds of detecting AA were 1.90×10^{-6} and 1.56×10^{-6} v/v for control and Kir2.1-off mice, respectively (Fig. 1d-i). Using *p*-values to identify the first concentration to elicit a noticeable increase in odor port investigation, we found that Kir2.1-off and control mice both have significantly increased investigation at 1×10^{-6} v/v for AA and HPO (Fig. 1d-ii and Supplementary Fig. 1b).

We performed additional evaluation of detection threshold using a Go/No Go test [21]. Water-restricted animals were trained to associate an odor with water reward then tested with lowered concentrations of the trained odor. From this test, we determined that the thresholds of detecting AA were 6.64×10^{-6} and 7.88×10^{-6} v/v for control and Kir2.1-off mice, respectively (Fig. 1e). The threshold values were slightly higher than those obtained from dishabituation assays, but at the same order of magnitude. This was consistent with our previous findings and might reflect a requirement for the mice to decide whether or not to lick the water spout [21]. Taken together, neuronal silencing during early postnatal development did not alter odor sensitivity in mice. Moreover, the animals were able to learn the association between odors and reward during the Go/No Go

training, suggesting that learned valence association was not affected either.

Kir2.1-off mice exhibit normal odor discrimination and learning

We next examined whether neuronal silencing caused the mice to lose their ability to discriminate odorants. Specifically, we aimed to test the animals' innate ability to discriminate odors without prior exposure. To achieve this goal, we adopted the cross habituation assay using PROBES [21]. This assay exploits the animal's natural tendency towards habituation following repeated exposure to the same stimuli carrying no apparent value, and novelty seeking behavior when a new stimulus is presented after habituation (Fig. 1f). We measured the duration of odor source investigation and normalized the values to that during the control (no odor) period to derive normalized port investigation (NPI) values [21] (also see Methods). These NPI values allowed us to compare among animals with varied individual behavior readout. We then used ΔNPI, the difference between NPI values for the novel and habituated odors, to measure discrimination between the odors. For eight pairs of mono-molecular odorants tested, the Kir2.1-off mice could discriminate them all (Fig. 1g). The scores for the Kir2.1-off mice were higher than those of the controls for some odors but not the others. None of the differences were statistically significant. Thus, the Kir2.1-off mice were not deficient in discriminating odors under naïve conditions.

Finally, we tested odor discrimination and associative learning ability in Kir2.1-off mice with the reinforced two-choice assay. In this assay, water-restricted mice learned to

distinguish a pair of odors and associate them with the spatial location of water ports in order to receive water reward [21,22]. The assay not only required the animals to discriminate odors, but also assign valence to the odors. Both control and Kir2.1-off mice achieved ~90% success rate after training to discriminate a pair of mono-molecular odors, amyl acetate and heptanal (Fig. 1h), and between a pair of complex odors lemon and maple (Fig. 1i). In tests using lower concentrations of odors, we observed similar decline in accuracy between the two groups (Fig. 1h, i). These results indicated that the Kir2.1-off mice not only could discriminate odors, but also could recognize individual odors and associate them with the correct water ports. Importantly, the Kir2.1-off mice were able to assign valence to odors during learning. Taken together, these results showed that the Kir2.1-off have no deficiency in odor discrimination, recognition and valence association.

Mismatch between OSN and mitral/tufted cells by altered neural activities

In wildtype mice, individual olfactory glomerulus is innervated by OSN axons expressing the same odorant receptor and by the primary dendrites of mitral/tufted cells (Fig. 2a-i). The convergent pattern provides a structural basis to transmit odor information. Suppressing spontaneous activities during the critical period have a profound impact on the convergent projection patterns of the OSNs. It was therefore surprising that suppressing spontaneous activity during early postnatal period did not ostensibly perturb olfactory function. It was possible that the change in OSN axon projection patterns did not alter the specificity of connection between OSNs and the mitral/tufted cells. In one

scenario, mitral/tufted cell dendrites are connected to OSNs regardless of the odorant receptors they express as long as they are in the same glomerulus (Fig. 2a-ii). It was also possible that the connection between sensory neurons and postsynaptic mitral cells was specified by molecular identities independent of spatial locations. In this scenario, axons expressing the same OR may be matched to the same mitral cell even though they are distributed into many glomeruli (Fig. 2a-iii, iv). The latter scenario would suggest the specific connection between OSNs and mitral/tufted cells could be maintained.

We noticed that in the Kir2.1-off mice axons expressing the same receptor were more concentrated in compartments within the glomeruli, with their terminal zones smaller than those observed in controls (Fig. 2b). If the dendrites of mitral cells were to match the axons of a given OR identity, we would expect a similar compartmentalization of dendritic trees. Thus, we quantified the level of compartmentalization of both axons and dendrites. We estimated the fractions of a glomerulus that could be innervated by a single type of axons in the Kir2.1-off mice carrying the *M72-IRES-tauGFP* allele. We used antibodies against GFP to label M72 axons and stained against olfactory marker protein (OMP) or NCAM to label the glomeruli [23,24]. In control mice, glomeruli innervated by the M72 axons were filled with GFP expressing fibers and exhibited near complete signal overlap between GFP and OMP, or GFP and NCAM (Fig. 2b-i, ii and Supplementary Fig. 2a-i-ii). In Kir2.1-off mice, many glomeruli receiving M72 fibers contained regions that were OMP+ (Fig. 2b-iii, iv) or NCAM+ (Supplementary Fig. 2a-iii, iv) but GFP-, indicating that the glomeruli containing the M72 axons were innervated by axons

expressing other receptors. Quantitative analysis revealed that glomeruli exhibited varied levels of innervation by the *GFP*-labeled axons for M72-expressing neurons (Fig. 2b-v and Supplementary Fig. 2b) even though the glomerular size remained constant (Fig. 2b-vi).

If the mitral cell dendrites were to match the axons, their projection pattern must be compartmentalized as well. To compare the level of compartmentalization, we analyzed glomerular occupancy by OSN axons and by mitral cell dendrites (Fig. 2c, d). To distinguish the two patterns, we applied a series of spatial filters of increasing sizes to tile the glomeruli and quantified the number of filters containing fluorescent signal (Fig. 2c, d). As filter size increased, glomerular occupancy increased and eventually reached 100% when the filter reached the size of the glomerulus. This rate of increase was fast for projections that distributed widely, but slow for those concentrated in small areas. This analysis showed that the axons from Kir2.1-off mice were compartmentalized. At filter size of 6 pixels, these axons occupied ~40% of the glomeruli compared to 100% in the control (Fig. 2c-iii, iv). The dendrites of the mitral cells, in contrast, did not project to more than one glomerulus. Within the glomerulus, they projected broadly into all parts of the glomeruli (Fig. 2d) in both wildtype and Kir2.1-off mice. They showed identical distribution and the same rates of increase with filter size (Fig. 2d-iii, iv). The mismatch between the axon and dendritic projection patterns indicated that in the Kir2.1-off mice, OSNs expressing a particular OR were connected with different mitral cells and vice versa. Individual mitral cells were likely to receive input from multiple receptor types.

Spontaneous activity of the OSNs is required for innate odor recognition

If spontaneous activity during early development is not required to enhance odor detection and discrimination, does it serve a specific function. We hypothesized that it might be required to establish innate attraction and aversion behaviors elicited by odors. We therefore tested innate odor preference in the Kir2.1-off mice using with the PROBES system [21]. This assay exploited the animal's natural tendency to investigate a stimulus. We measured the duration of odor source investigation and compared it to the no odor period. The level of investigation indicated odor preference [21]. Control mice exhibited increase frequency and duration in sniffing the odor port at the presentation of peanut butter odor or mouse urine (Fig. 3a). The increase in investigation sustained into the second and third presentations. In contrast, when odors aversive to the animals were presented the first time, control mice exhibited approaches to the odor port at a level similar to that of air control (Fig. 3b). At the second presentation, we observed marked reduction in investigation of the odor port. It was likely that at first odor presentation, investigative behavior was driven by two conflicting drives: risk assessment (approach) and avoidance. We thus used the reduction at the second odor epoch to measure avoidance (see Methods).

From this assay, it was clear that odors of peanut butter and mouse urine elicited strong attraction when compared with monomolecular odors that were generally considered as

neutral (Fig. 3c). In contrast, the Kir2.1-off mice did not exhibit attraction to food and conspecific urine odors (Fig. 3a, c). The level of investigation of the odor port was comparable to those of the neutral odors and did not sustain after the first presentation. Control mice also showed aversion towards odors considered as aversive, including coyote urine, 2-phenethylamine (PEA), 2-methylbutyric acid (2-MBA) and isoamylamine (IAMM). The Kir2.1-off mice, on the contrary, continued to investigate the aversive odor at a level approach that to the neutral odors (Fig. 3b, d). These results indicated that silencing OSNs during early postnatal development impaired the ability of the mice to recognize the valence of these ethologically relevant odors.

Altered central representation of innately recognized odors

Odor information is processed by multiple pathways in the brain. Whereas the anterior olfactory nucleus and the piriform cortex are involved in channeling odor information regardless of their valence, other brain areas were associated with odor valence. Positive valence is generally associated with the posterolateral cortical amygdaloid area (PLCo), medial amygdaloid nucleus (postdorsal area; MePD and postventroral area; MePV), and the ventrolateral nucleus of the ventral medial hypothalamus (VMHvl). Negative valence is generally associated with the bed nucleus of stria terminalis (BST), the anterior hypothalamic area, anterior part (AHA) and the ventral medial hypothalamus (VMH). We therefore examined the activation of these brain regions by the innately recognized odors. We performed immunofluorescence staining using antibodies against phospho-S6

(pS6) ribosomal protein after exposing the animals to a specific odor [25]. 2-MBA activated the BST, AHA and VMH over background when compared with no stimulus in the control mouse brains (Fig. 4a, c). However, we did not observe above background activation in the Kir2.1-off mouse brain. Another aversive odor, PEA, showed similarly reduced activation of these brain regions of the Kir2.1-off animals (Supplementary Fig. 3). We also observed that the PLCo, MePD, MePV and VMHvl were activated by female urine in the control mice but not the Kir2.1-off mice (Fig. 4b, d). These observations suggested that the Kir2.1-off mice had altered representation of the odors in brain regions associated with valence.

Exposure to aversive odor during critical period alters innate odor recognition

The loss of innate odor preferences following neuronal silencing during an early period of postnatal development was surprising. It suggested that the neural circuits processing innate valence were plastic during development. We hypothesized that this developmental plasticity would allow early olfactory experience to influence odor-evoked innate responses later in life. We chose the PEA as an aversive odor to test this hypothesis because it specifically activated the TAAR4 receptor, which is necessary for PEA-induced aversion [10,11].

We raised pups in an environment infused with PEA during the first two postnatal weeks (Fig. 5a). Following another seven weeks without exposure, we tested the animals'

response to PEA (Fig. 5a). To test whether the influence of PEA was restricted to a specific time window, we exposed another group of animals to PEA between postnatal day 24 and 38, followed by testing at 9 weeks of age (Fig. 5b). To determine the odor specificity of this change in responses, we also tested behavioral response to IAMM, which elicited innate aversion but was not exposed to the animals during these periods.

Compared to the control mice that showed aversion to PEA, the P0 - P14 treated animals did not exhibit aversion to PEA (Fig. 5c). These mice, however, still exhibited aversive response to IAMM (Fig. 5d). The timing of PEA exposure also had a profound impact on odor aversion in adults. In contrast to the early postnatally exposed mice, animals that had late exposure to PEA exhibited aversion to both PEA and IAMM (Fig. 5c, d).

Altered odor representation by early odor exposure

We next examined the activation of brain regions associated with innate odor-triggered behaviors in animals exposed to PEA during the critical period. We found that in mice that were exposed to PEA during the first two weeks after birth, PEA no longer activated BST, AHA, BLA and the MePV above background (Fig. 6a). In contrast, in mice exposed to PEA after the critical period, these brain areas were activated by PEA (Fig. 6). These findings were consistent with the change of innate aversion toward PEA.

Neural activities influence axon projection pattern of TAAR4 receptor

Temporary suppression of action potentials during early postnatal development did not alter odor detection, discrimination and associative learning, yet abolished innate odor preference. Early exposure to an aversive odor similarly disrupted innate odor recognition. The patterns of activation in the brain suggested that the innate neural circuits that linked specific odors with attraction or aversion were altered. We, therefore, investigated how neural activities influence the neural circuits and lead to altered innate odor recognition.

Odor valence could be conveyed by specific parts of the olfactory bulb. For example, the dorsal bulb was shown to be required for conveying aversive information of aversive odors [13]. Alternatively, but not mutually exclusively, a highly specific link between the odorant receptors, a set of mitral/tufted cells, and their downstream targets could be established through genetically specified hardwiring regardless of the spatial locations where the receptor neurons project to. In previous studies, we have shown that suppression of neural activity during early development caused the olfactory axons expressing the same receptor to innervate multiple glomeruli [14,15,18,26]. We also found that the OSNs projected to the same dorsal-ventral and anterior-posterior position of the olfactory bulb where wildtype axons innervated, suggesting that the general topology of OSN innervation remained intact and the OR gene expression was maintained. However,

it was not known whether the broadened projection patterns also applied to receptor neurons that transmit identity information of innately recognized odors.

We, therefore, examined whether the OSNs detecting an aversive odor maintain their projection specificity. We performed immunofluorescence staining using antibodies against TAAR4 [27], which detected PEA and was required for aversive response to PEA [7]. We found that in the Kir2.1-off mice the axons expressing TAAR4 projected to more glomeruli than the wildtype mice (Fig. 7a; 1.86 ± 0.38 and 5.33 ± 2.34 glomeruli per dorsal OB for control and Kir2.1-off, respectively). Nevertheless, the glomeruli receiving TAAR4 projection were located in the dorsal and medial olfactory bulb, in the same general region as the wildtype TAAR4 glomeruli.

We next performed the same experiments on mice that were exposed to PEA during first two postnatal weeks. We found that PEA exposure also led to divergent projection of TAAR4 expressing axons (Fig. 7b). TAAR4 axons were found on average 5.22 ± 1.64 glomeruli per OB, significantly more than in the control mice (2.53 ± 0.69; Student *t*-test, $p = 0.0016$). Moreover, the number of TAAR4 glomeruli in mice exposed to PEA between P24 and P38 was indistinguishable from the controls (3.0 ± 0.89, $p = 0.376$).

We also stained the sections using antibodies against the receptor MOR28, which did not respond to PEA [28]. The number of glomeruli innervated by MOR28 OSNs was not affected by the PEA exposure (Fig. 7c, 2.14 ± 0.38, 2.17 ± 0.41 and 2.09 ± 0.30 glomeruli per OB for control, P0 - P14 PEA exposure and P24 - P38 PEA exposure

respectively, $p = 0.50$ and 0.39). These observations suggested that the activation of the dorsal bulb was not sufficient for conveying aversive signals. It was likely that the divergent connection of TAAR4 axons to the glomeruli led to altered odor representation.

Discussion

Plasticity in an innate sensory circuit

The recognition of ethologically relevant odors by naïve animals ensures the natural tendency of the animals to engage in social interactions, find food and avoid predator can be properly triggered. The discovery that the circuit for innate odor perception is malleable shows that circuits processing innate responses are not fully hardwired in the mammalian brain. They are subject to influence by both spontaneous and experiential activities. Importantly, the plasticity is observed only during early postnatal period, the same time window during which developing olfactory projection patterns, which is subject to influences by different perturbations and can recover when perturbations are removed [17-19]. These findings show that as a general principle, neural activities regulate the development of sensory circuits in the mammalian nervous system.

The role played by neural activities in shaping the olfactory circuits appears different from that of other sensory systems. Visual input, for instance, is required for the

segregation of ocular-specific input in the lateral geniculate and in the cortex [29,30]. Dark rearing delays the binocular segregation, as well as the closure of the critical period in the visual cortex. In contrast, spontaneous activities, not odor exposure, is required for the convergence of axons [15]. Enhanced stimulation by an odor, on the other hand, leads to broadened axon projection and alters the innate valence of the odor.

The molecular mechanisms that specify connections between the OSNs and the mitral/tufted cells are not well understood. A recent study demonstrates that the firing patterns of OSNs are associated with the odorant receptors they express [16]. Moreover, the firing patterns are associated with the glomeruli identities. It is possible that suppression of spontaneous activity of the neurons alters the expression of specific guidance and cell adhesion molecules in the OSNs, leading them to innervate different glomeruli. Similarly, persistent stimulation by an odorant could affect the expression of these genes by overriding the activity patterns dictated by the ligand-independent activities of odorant receptors [14].

Glomerular convergence, odor sensitivity and discrimination

A previous study examining the mice with ectopic expression of Kir2.1 have reported olfactory defects [31]. The reported observations were likely caused by the continuous expression of Kir2.1 channel in the OSNs, which not only suppressed spontaneous activities of the neurons but also reduced odor-evoked responses. In our study, by

contrast, the Kir2.1-off mice were fed with DOX after the critical period to restore neural activities. These experiments were not complicated by the effect of suppressed neuronal responses.

In the Kir2.1-off mice, the olfactory map was imprinted from the early developmental stage. The axon projection patterns were permanently altered from single receptor type convergence into a pattern with individual glomerulus receiving innervation from multiple receptor type axons. These mice provided a unique opportunity to test the contribution of the single receptor type convergence on odor sensitivity, discrimination and association. In wildtype mice, errors in the convergence of axons expressing the same odorant receptor into their perspective glomeruli are rarely observed. In both wildtype and in mice with genetic manipulations to alter axon projection patterns, ectopic glomeruli can be pruned during development [17,18,32]. A robust mechanism that maintains the convergent projection pattern has likely been selected during evolution to serve important functions, including odor recognition and discrimination. It is therefore surprising to find that Kir2.1-off mice do not have major defects in odor detection, discrimination and association. The single receptor type convergence does not appear to be required for olfactory function. In light of its role in innate odor perception (see below), we reason that one function of the convergent olfactory map is to provide consistency in odor perception among individuals. Alternatively, the convergent map may offer an advantage in fine odor discrimination that is not captured by our current study.

The role of axon convergence in innate odor perception

Our results demonstrate the importance of single glomerulus axon convergence in providing a substrate for innate odor recognition. Perturbing the convergent pattern, through either transient silencing of the OSNs or exposure to the odorant during the critical period, alters the innate behavioral responses. These results reaffirm the previous observations that OSN axons and mitral cell dendrites develop independently [18]. Furthermore, it extends the previous studies by showing that it is unlikely to be a strict molecular identity code matching OSN axons with mitral cell dendrites as the two show different compartmentalization patterns in the glomeruli. This observation is consistent with a recent study showing that mitral cell dendrites mostly project to the spatially proximal glomeruli [33]. Taken together, these results indicate that glomerular convergence is critical for innate coding of odor identity. It is likely that specify sets of glomeruli and the mitral/tufted cells innervating these glomeruli carry information about the identities of innately recognized odors. This stereotyped connection provides a substrate for the alteration of innate preference by altering the projection patterns of OSN axons.

Notably, although OSN axons project to multiple glomeruli in the Kir2.1-off as well as in odor-exposed mice, they maintain their general dorsal-ventral and anterior-posterior position in the bulb. For odors whose receptor neurons innervate the dorsal area of the glomeruli, this broad spatial target is not sufficient to assign negative valence to the odors

and generate aversive responses, even though the dorsal bulb is shown to be required to convey negative valence information for odorants [13].

How is valence information encoded for the innately recognized odors? It is likely that the activation of specific set of glomeruli activates the mitral/tufted cells that are connected with brain centers that control appetitive or aversive behaviors (Fig. 8a). Perturbation of the projection pattern of OSN axons disrupt this association. Our experiments demonstrate that the mitral cells maintain connection with individual glomeruli without discriminating the different types of axons. One possibility is that the mitral cells also specific the connections with downstream behavioral centers. Divergent innervation of glomeruli by could activate additional mitral/tufted cell population and the activation of brain centers that drive opposing behaviors (Fig. 8b). This antagonism may lead to the loss of innate preference associated with specific odors.

An alternative, but not mutually exclusive scenario is that the change in OSN projection patterns leads the recoding of odor identity (Fig. 8c). Odor identities are represented by population responses of the mitral/tufted cells. The patterns of activation are not strictly determined by the direct relay from activated glomeruli but are the result of interactions among cells within the neuronal network. Innately recognized odors are represented by specific sets of neurons whose connections to the valence centers are strongly biased toward one appetitive or aversive pathway. This association, while genetically specified, is flexible and can also be modified.

Developmental perturbations could alter the way odor identities are represented by activating a different set of neurons in the olfactory pathway. An altered representation would eliminate the biased activation of brain centers driving appetitive or aversive behaviors (Fig. 8c). This model is consistent with emerging evidence that suggests innate preference is context dependent, and has strong interactions among olfactory pathways [34,35]. It is also consistent with evidence that ethologically relevant odors are encoded similarly as ordinary odors in cortical structures thought to encode innate preference [36].

Methods

Animals

The *tetO-Kir2.1-IRES-tauLacZ, OMP-IRES-tTA, M72-IRES-tauGFP,* (Jackson laboratory, stock number 009136, 017754, 004946, and 006678, respectively) were described previously [15,20,28,37]. For early odor exposure experiments, CD1 (Jackson laboratory, stock number: 003814) animals were used. All animals were maintained in Lab Animal Services Facility of Stowers Institute at 12:12 light cycle and provided with food and water *ad libitum* except animals for two-choice and Go/No Go experiments. All behavior experiments were carried out during the dark cycle of the animals under red or infrared light illumination. Experimental protocols were approved by the Institutional Animal Care and Use Committee at Stowers Institute (protocol 2019-102) and in compliance with the NIH Guide for Care and Use of Animals.

Compound heterozygotes carrying the *OMP-IRES-tTA* and the *tetO-Kir2.1-IRES-taulacZ* alleles were weaned at P21 and fed with diet (TestDiet) containing 20mg/kg doxycycline (DOX) for more than 6 weeks prior to any experiments unless otherwise indicated (Kir2.1-off). Single-allele littermates of the Kir2.1-off mice and wildtype C57BL/6J (Jackson laboratory, stock number: 000664) strain mice (referred to as B6) were subject to the same treatment and served as controls.

Odor delivery with olfactometer

Odor delivery was controlled by an automated olfactometer with custom written software developed in the National Instrument Labview programming environment as described previously [21,38]. Odorant chemicals are including: Amyl acetate (Abbr: AA), Hexanal

(Abbr: HXH), 2-Pentanone (Abbr: PTO), Valeraldehyde(Abbr: VAH), Butyl acetate (Abbr: BAE), 2-Heptanone (Abbr: HPO), Methyl butyrate (Abbr: MPE), Methyl propionate (Abbr: MPE), R(-)-Carvone (Abbr: (-)Car), S(-)-Carvone (Abbr: (+)Car), Methyl caproate (Abbr: MCE), Methyl valerate (Abbr: MVE), 2-Hexanone (Abbr: HXO), Heptanal (Abbr: HPH), Eugenol (Abbr: EUG), 2-Methylbutyric acid (Abbr: 2-MBA), 2-phenylethylamine (Abbr: PEA) , isoamylamine (Abbr: IAMM) and were purchased from MilliporeSigma and freshly prepared in mineral oil at desired concentration. sFemale mouse urine (fresh collected from C57BL/6J mice, Abbr: FU), Male mouse urine (fresh collected from C57BL/6J mice, Abbr: MU), Coyote urine (Abbr: CU), Peanut butter (Jif Extra Crunchy, Abbr: PB), Maple flavor (Frontier natural products co-op, Abbr: Maple), Lemon flavor (Frontier natural products co-op, Abbr: lemon) were used at original concentration.

Cross habituation test

Habituation tests were same as previously described [21]. 2-4 months old mice were used for cross habituation experiments. Each experimental group contained 6-14 animals. Unless otherwise stated, all animals were naïve to the testing odors and exposed to the same odor once. Each animal was tested with a total of 4 odors (2 pairs) in 2 separate experiments with at least one week between tests. After being habituated to the testing environment for half an hour, the animals were put into a 20 x 20 cm chamber for behavioral experiments. The chamber had a nose cone on one of the side wall 5 cm above the base plate. Odors were delivered through the nose cone by the olfactometer. A vacuum tube connected on the opposite wall of the nose cone provided an air flow to remove residual odors after odor delivery. Pure odorants were diluted into mineral oils at 1:1000 (v/v) in most cases. 10 ml/min air flow carried the saturated odor out from the odor vial and was further diluted into a 90 ml/min carrier air to make the final dilution to 10^{-4} (v/v). Delivery time, concentration and sequence of odor delivery were controlled by

the olfactometer. Investigation of odor source was registered by infrared beam breaking events and recorded by the same software that controlled the olfactometer.

In each trial an odor was delivered for 1 minute followed by 4 minutes of carrier air. Mice were first habituated with eight trials of air followed by testing odors. Investigations to the odor port during the control air presentation (T_{Air}) or odor presentation (T_{Odor}) were recorded. After the mice had been habituated to the first odor (5 trials), a second odor was presented 3-5 times. In a typical test, mice habituating to the test chambers over the multiple sessions of background air led to decreased T_{Air}. The presentation of an odor elicited an increased T_{Odor}. Repeated presentation of the same odor led to habituation, which was reversed by the test odor if it was perceived as novel. No increased investigation was expected if the test odor was perceived similarly to the habituating odor. Normalized NPI for individual trial was calculated by dividing T_{Air} or T_{Odor} by the average duration of odor port investigation during the background air $T_{Ave.Air}$ ($T_{Ave.Air} = \sum T_{Air} / N$). Distance between two odors in behavioral test was calculated as the difference in normalized exploration duration:

$$\Delta NPI = \frac{T_{odor2.1} - T_{odor1.5}}{T_{Ave.Air}} \times 100$$

Where $T_{Odor2.1}$ was the exploration duration for the first session of Odor 2 (the testing odor) and $T_{Odor1.5}$ was the exploration time of the 5th (last) session of Odor 1 (the habituating odor). As such, ΔNPI is the difference between the investigation time of a novel odor and that of the habituated odor, expressed as the percentage over the average exploration time during air presentation. Pair-wise *t*-test was performed for statistical analysis.

Innate odor preference test

The experiments were carried out similarly as the cross-habituation assay with modification of odor presentation period. Odor was delivered for 5 minutes in each trial with a 5-minute interval. After four trials of air (over mineral oil vial) presentation, a testing odor was presented 4 times. In a typical test, mice habituating to the test chambers over the multiple sessions of background air led to decreased T_{Air}. The presentation of an odor elicited investigations and measured as T_{Odor}. If the odor is attractive to the animal, an increased in T_{Odor1} is expected to be higher than that for a neutral odor as both novelty seeking and attraction drive the investigations. If the odor is aversive to the animal, a smaller increase or even decrease T_{Odor1} is expected as the mixed result of novelty seeking (risk assessment) and avoidance, while the T_{Odor2} is expected as the aversion only because the novelty is habituated quickly while the avoidance persists longer. We define the following indices:

$$\text{attraction index} = \frac{T_{Odor1} - T_{Air4}}{T_{Ave.Air}} \times 100$$

$$\text{aversion index} = \frac{T_{Air4} - T_{Odor2}}{T_{Ave.Air}} \times 100$$

Dishabituation test for threshold determine

The trial sequence used to measure detection thresholds is the same as previous described [21]. After the 8 initial air presentations, an odor was presented at the lowest concentration (10^{-8} v/v). An air presentation and an odor presentation interleaves in the test with the odors being presented at increasing concentration. The *p*-values of normalized ΔNPI between air and the odor presentation were calculated.

ΔNPIs at different odor concentrations (x) were fitted with Nonlinear Least Squares method using Weibull psychometric function in MATLAB:

$$SR = A - (A - g) * e^{-(\frac{kx}{t})^b}$$

where

$$k = -[\ln(\frac{A - a}{A - g})]^{\frac{1}{b}}$$

A is the maximum performance, b is the steepness of the function, and a is the threshold concentration. The parameter g is the false alarm rate which is set at 0%.

Two alternative choice test and Go/No Go test

Animals were maintained on a water restriction regimen with 1.5 ml of drinking water per day for at least one week before training. Food was available *ad libitum*. A decrease in body weight of 10-15% from the original was normally observed. All the training and testing were performed during the dark light cycle 24 hours after the last water feeding.

For two alternative choice (two-choice) test, water restricted animals were introduced into a 20 x 20 cm behavioral box that contains three nosecones on one side of the wall. Each nosecone contains a pair of infrared emitter and receiver and the nose poke events were registered as the breaking of IR beam. The central port delivers an odor puff whereas the two side ports delivered water. Delivery was triggered when the animal poked in. Odor delivery, nose poke event registration and the water reward were controlled by the olfactometer. In initial training, animals were presented with a single odor that was associated with a fixed water port. Once the animals learned to go to the water port upon odor delivery in the odor port, they were subject to two-choice training.

Two odors were delivered in a pseudo random sequence and water reward was contingent upon the animal correctly associating the odor with the appropriate water port. If the animal chose the correct port, 0.05 ml water was released as reward for the right choice. Otherwise, no water was given. The animals were considered to have learned the behavior paradigm if the success rate reached 80%. Success rate (SR) was calculated as:

$$SR = \frac{P_{[A/A]} + P_{[B/B]}}{P_{total}} \times 100$$

where $P_{[A/A]}$, $P_{[B/B]}$ and P_{total} were the number of pokes into A water port upon delivery of odor A, the number of pokes into B water port upon odor B and the total number of nose pokes into the odor port, respectively. Upon reaching criteria, the concentrations of both A and B were gradually decreased for the 2-choice test.

Go/No Go assay was applied for odor threshold detection as a second method as described previously [21]. Basically, water deprived animals were trained to associate an CS+ odor (amyl acetate) with water reward by poking into the nose cone and licking the waterspout when the CS+ odor delivered. A CS- presentation (air) was coupled with a mild electric shock (30v, 0.7sec), when the mouse licked the waterspout. Success rate (SR) was calculated as:

$$SR = \frac{P_{CS+} + NP_{CS-}}{P_{CS+} + NP_{CS+} + P_{CS-} + NP_{CS-}}$$

where P_{CS+} and NP_{CS+} were the number of licking and non-licking events for the CS+ odor, P_{CS-} and NP_{CS-} were number of the licking and non-licking events for the CS- odor respectively. After the animals were considered to have learned the behavior paradigm when success rate reached 90%, we measured SR of licking events at different

concentrations of AA. The measured performance values also were fitted by the Weibull psychometric function with the parameter *g* was at the chance level (50%).

Dendritic knob recording on M72-GFP OSNs

Cell-attached loose patch clamp recordings were done on intact sheets of dissected olfactory epithelium (OE). During the recording the epithelium was perfused continuously with oxygenated ACSF and Ringer's solution in a custom-made recording chamber. The dendritic knobs of the M72-GFP neurons were identified and visualized using Zeiss LSM510 with excitation at 488 nm. Recordings were made using glass pipettes with tip size of less than 1µm and resistance of 10-25 MΩ. The recording electrodes were filled with Ringer's solution. The action potentials were acquired using Multiclamp 700A (Molecular Devices) and were digitized at 10 kHz by Digidata 1440A (Molecular Devices). The data was recorded and analyzed using pClamp10 software (Molecular Devices).

Electro-olfactogram (EOG) recording

Half-brain preparations were freshly made by bisecting the head through the midline to expose the OE. A glass pipette (1MΩ resistance) filled with 1X PBS was used in the EOG recording. Amyl acetate was prepared at 1:100 dilution and delivered at 50 ml/min flow rate in 50 ml/min moisturized carrier air. Total flow rate was maintained at 100 ml/min during the experiment. Odor was delivered for 0.5 second to the epithelium followed by a 20 seconds interval. Average response from 4 trials was used in quantification. Signal was amplified with Axon CyberAmp320 (Molecular Devices) and digitized with Axon Digidata 1320 (Molecular Devices). The pClamp10 software (Molecular Devices) was used for data acquisition and processing. Each half brain was recorded for no more than 15 minutes to ensure the viability of the olfactory sensory neurons.

Immunofluorescent staining and dye labeling

The mice carrying the *M72-IRES-GFP* allele were crossed into the *OMP-IRES-tTA* / *tetO-Kir2.1-IRES-taulacZ* compound heterozygotic background and treated with DOX to obtain control or Kir2.1-off mice. Immunofluorescent staining was carried out using 14-16 µm olfactory bulb cryosections or 50µm olfactory bulb sections with vibratome (Leica VT 1000 S) prepared from animals perfused with 4% paraformaldehyde (PFA). Sections were washed in 1X PBS, permeabilized in 1X PBS containing 0.1% TritonX-100 (PBST) and blocked in 1% skim milk dissolved in PBST. Rabbit or rat anti-NCAM (Millipore, Cat#: ABN2181-100UG, 1:400), chicken anti-GFP (Abcam, Cat#: ab13970-100, 1:400), Rabbit anti-OMP (Wako, Cat#: 544-10001, 1:400), Rabbit anti-MOR28 (Barnea Lab, 1:500), Rabbit anti-Phospho-S6 (Ser235/236, Cell Signaling, Cat#: 4854, 1:1000) and guinea pig anti-TAAR4 (Barnea Lab, 1:500) antibodies in PBST were used to stain the section overnight at 4oC or room temperature. Alexa Fluor conjugated secondary antibodies (Donkey anti-Rabbit 488, Thermo Fisher Scientific, Cat#: R37118; Goat anti-Guinea Pig Alexa Fluor 488, Thermo Fisher Scientific, Cat#: A-11073; Goat anti-Guinea Pig Alexa Fluor 568, Thermo Fisher Scientific, Cat#: A-11075) were diluted to 1:1000 in PBST for staining overnight. TOTO-3 (Thermo Fisher Scientific, Cat#: T3604) or DAPI (Thermo Fisher Scientific, Cat#: D1306) was used for nuclear staining.

Mitral cell dendritic tuft labelling was performed by iontophoresis method (Stimulus isolator A360, World Precision Instrument. 2.5 µA, 2 Hz, 5-10 min) of biotinylated dextran amines (BDA, 3000 MW, Life Technology, Cat#: D7135) into the dorsal and median of mitral cell layers in olfactory bulb. Animals were perfused with 1X PBS with 4% PFA 12 hours after labeling. The olfactory bulb was dissected and post-fixed with 4% PFA at 4ºC overnight, and then sectioned at 50µm thickness with vibratome (Leica VT 1000 S). The sections were then stained with 2ug/ml streptavidin Alexa Fluor 568 conjugate (Life Technology, Cat#: S11226) and DAPI.

All images were taken on a Zeiss LSM510, LSM700 or Zeiss LIVE confocal system. For co-localization analysis, an image stack was scanned using multi-track method and a

maximal projection of the stack was obtained. Co-localization coefficient was calculated as the percentage of GFP positive pixels over the NCAM positive pixels within a glomerulus. For mitral cell labeling, Z-stack confocal images were obtained for dendrite tracing. For interneuron staining, cells in the glomeruli layer with positive staining were counted using ImageJ. Glomeruli numbers were calculated by DAPI staining.

Glomerulus occupancy were calculated using a custom-written script in ImageJ. Images were Z projected using maximum projection method in ImageJ and a hard threshold was applied to obtain binary images. After the glomerulus is circumscribed, a series of spatial filters with increasing pixel sizes (1-20 pixels) were applied to tile the glomeruli. Each filter containing a positive signal is considered to be occupied. Glomerular occupancy was quantified by computing the percentage of filters with a signal in the circumscribed glomerulus.

Phospho-S6 mapping of odor-evoked activity

For phospho-S6 staining, animals were single housed and habituated in home cages for seven days with a glass vial covered with a plastic cover, which was punched with seven holes for odor evaporation and avoiding physical contact to chemicals. For habituation, a small piece of cotton nestlet soaked with 500 µl mineral oil was put inside the vial. Vials were changed every day at one hour after light cycle. In day eight, new glass vial with cotton nestlet soaked with 500 µl 2-phenylethylamine (PEA), 2-methylbutyric acid (2-MBA) at $1:10^3$ dilution in mineral oil, or freshly collected male or female urine was added in the home cages. One hour after odor stimulation, mice were sacrificed and intracardiac perfused with 4% PFA. The mouse brains were dissected and then post-fixed with 4% PFA overnight at 4ºC.

The phospho-S6 immunochemistry histology was performed based on the published protocol [25] with some modifications. The entire brain was cut into 50 µm thick serial sections using a Leica vibratome (VT1000S). Rabbit anti phospho-S6 antibody (1:1000

dilution) and the 3-p peptide (25nM, synthesized by United Peptide and has the sequence biotin-QIAKRRRLpSpSLRApSTSKSESSQK, where pS is phosphoserine) in 1X PBST were used at 4ºC overnight. Tiled images were acquired using Olympus VS120 Virtual Slide Microscope, or PE Ultraview spinning disk confocal microscope (PerkinElmer) which were stitched together using the Volocity software (PerkinElmer). Different brain nuclei were identified based on the brain atlas (The Mouse Brain Stereotaxic Coordinates, third/fourth edition) [39,40]. The pS6 immuno-positive neurons were counted using ImageJ. For quantification the two sides of the brain were treated independently and the following numbers of sections were used: anterior hypothalamic area, anterior part (AHA), 4 sections at -0.85~-1.05 mm from Bregma; medial amygdaloid nucleus (postdorsal area; MePD and postventroral area; MePV) and ventromedial hypothalamic nucleus (ventrolateral area; VMHvl), 5 sections between -1.35~-1.60 mm from Bregma; hypothalamic nucleus (VMH) in the 2-MBA case, 4 sections between -1.80~-2.00 mm from Bregma; bed nucleus of the stria terminalis (BST), 3 sections between 0.10~0.25mm from Bregma; anterior cortical amygdaloid area (ACo), 4 sections at -1.00~-1.20mm from Bregma; posterolateral cortical amygdaloid area (PLCo), 5 sections at -1.35~-1.60mm from Bregma; paraventricular thalamic nucleus, anterior part (PVA), 4 sections at -0.25~-0.45mm from Bregma ; piriform cortex (Pir), 5 sections at -1.35~-1.60mm from Bregma; basolateral amygdaloid nucleus, anterior part (BLA), 5 sections at -1.10~-1.35mm from Bregma.

Early PEA exposure

For early odor exposure experiments, a piece of cotton nestlet soaked with 1 ml PEA (1:100 in mineral oil) in a glass vial was put inside the home cage. The odor vial was changed daily with fresh prepared PEA. For the P0-14, the home cage contains both mother and pups. After the odor stimulation period, the animals were raised regularly without the odor vials till 9 weeks for behavior and histology experiments.

Quantification and statistical analysis

All the statistics are conducted in Matlab or OriginPro. Data were expressed as means ± SEMs in figures and text. Group differences were analyzed using one-way Student *t*-test. Significance was defined as: * indicates $p < 0.05$, ** indicates $p < 0.01$, *** indicates $p < 0.001$. ns indicates $p > 0.05$.

Acknowledgments

We thank A. Moran and members of the Lab Animal Services at the Stowers Institute for technical assistance. We are grateful to Dr. P. Mombaerts for providing the *M72-IRES-tauGFP* mice, and Dr. G. Barnea for providing antibodies against TAAR4 and MOR28. We also thank valuable input from members of the Yu laboratory. The work is supported by funding from Stowers Institute and the NIH (R01DC008003, R01DC 014701 and R01DC016696).

Ethics declarations

Competing interests

The authors declare no competing interests.

References

1 Hensch, T. K. Critical period plasticity in local cortical circuits. *Nature Reviews Neuroscience* **6**, 877-888 (2005).

2 Hubel, D. H. & Wiesel, T. N. The period of susceptibility to the physiological effects of unilateral eye closure in kittens. *The Journal of physiology* **206**, 419-436 (1970).

3 Tye, K. M. Neural Circuit Motifs in Valence Processing. *Neuron* **100**, 436-452 (2018).

4 Buck, L. & Axel, R. A novel multigene family may encode odorant receptors: a molecular basis for odor recognition. *Cell* **65**, 175-187 (1991).

5 Liberles, S. D. & Buck, L. B. A second class of chemosensory receptors in the olfactory epithelium. *Nature* **442**, 645-650 (2006).

6 Greer, P. L. *et al.* A Family of non-GPCR Chemosensors Defines an Alternative Logic for Mammalian Olfaction. *Cell* **165**, 1734-1748 (2016).

7 Pacifico, R., Dewan, A., Cawley, D., Guo, C. & Bozza, T. An olfactory subsystem that mediates high-sensitivity detection of volatile amines. *Cell reports* **2**, 76-88 (2012).

8 Axel, R. Scents and sensibility: a molecular logic of olfactory perception (Nobel lecture). *Angew Chem Int Ed Engl* **44**, 6110-6127 (2005).

9 Ishii, K. K. *et al.* A Labeled-Line Neural Circuit for Pheromone-Mediated Sexual Behaviors in Mice. *Neuron* **95**, 123-137.e128 (2017).

10 Zhang, J., Pacifico, R., Cawley, D., Feinstein, P. & Bozza, T. Ultrasensitive detection of amines by a trace amine-associated receptor. *J Neurosci* **33**, 3228-3239 (2013).

11 Dewan, A., Pacifico, R., Zhan, R., Rinberg, D. & Bozza, T. Non-redundant coding of aversive odours in the main olfactory pathway. *Nature* **497**, 486-489 (2013).

12 Pérez-Gómez, A. *et al.* Innate Predator Odor Aversion Driven by Parallel Olfactory Subsystems that Converge in the Ventromedial Hypothalamus. *Current Biology* **25**, 1340-1346 (2015).

13 Kobayakawa, K. *et al.* Innate versus learned odour processing in the mouse olfactory bulb. *Nature* **450**, 503-508 (2007).

14 Nakashima, A. *et al.* Agonist-Independent GPCR Activity Regulates Anterior-Posterior Targeting of Olfactory Sensory Neurons. *Cell* **154**, 1314-1325 (2013).

15 Yu, C. R. *et al.* Spontaneous neural activity is required for the establishment and maintenance of the olfactory sensory map. *Neuron* **42**, 553-566 (2004).

16 Nakashima, A. *et al.* Structured spike series specify gene expression patterns for olfactory circuit formation. *Science* **365**, eaaw5030 (2019).

17 Tsai, L. & Barnea, G. A critical period defined by axon-targeting mechanisms in the murine olfactory bulb. *Science* **344**, 197-200 (2014).

18 Ma, L. *et al.* A developmental switch of axon targeting in the continuously regenerating mouse olfactory system. *Science* **344**, 194-197 (2014).

19 Wu, Y. *et al.* A Population of Navigator Neurons Is Essential for Olfactory Map Formation during the Critical Period. *Neuron* **100**, 1066-1082.e1066 (2018).

20 Feinstein, P. & Mombaerts, P. A contextual model for axonal sorting into glomeruli in the mouse olfactory system. *Cell* **117**, 817-831 (2004).

21 Qiu, Q. *et al.* Automated Analyses of Innate Olfactory Behaviors in Rodents. *PLoS One* **9**, e93468 (2014).

22 Uchida, N. & Mainen, Z. F. Speed and accuracy of olfactory discrimination in the rat. *Nat Neurosci* **6**, 1224-1229 (2003).

23 Keller, A. & Margolis, F. L. Immunological studies of the rat olfactory marker protein. *J Neurochem* **24**, 1101-1106 (1975).

24 Terkelsen, O. B., Bock, E. & Mollgard, K. NCAM and Thy-1 in special sense organs of the developing mouse. *Anat Embryol (Berl)* **179**, 311-318 (1989).

25 Knight, Z. A. *et al.* Molecular profiling of activated neurons by phosphorylated ribosome capture. *Cell* **151**, 1126-1137 (2012).

26 Zhao, S. *et al.* Activity-dependent modulation of odorant receptor gene expression in the mouse olfactory epithelium. *PLoS One* **8**, e69862 (2013).

27 Johnson, M. A. *et al.* Neurons expressing trace amine-associated receptors project to discrete glomeruli and constitute an olfactory subsystem. *Proceedings of the National Academy of Sciences of the United States of America* **109**, 13410-13415 (2012).

28 Barnea, G. *et al.* Odorant receptors on axon termini in the brain. *Science* **304**, 1468 (2004).

29 Wiesel, T. N. & Hubel, D. H. EFFECTS OF VISUAL DEPRIVATION ON MORPHOLOGY AND PHYSIOLOGY OF CELLS IN THE CAT'S LATERAL GENICULATE BODY. *Journal of Neurophysiology* **26**, 978-993 (1963).

30 Shatz, C. J. & Stryker, M. P. Ocular dominance in layer IV of the cat's visual cortex and the effects of monocular deprivation. *The Journal of physiology* **281**, 267-283 (1978).

31 Lorenzon, P. *et al.* Circuit Formation and Function in the Olfactory Bulb of Mice with Reduced Spontaneous Afferent Activity. *The Journal of Neuroscience* **35**, 146-160 (2015).

32 Zou, D. J. *et al.* Postnatal refinement of peripheral olfactory projections. *Science* **304**, 1976-1979 (2004).

33 Nishizumi, H. *et al.* Primary dendrites of mitral cells synapse unto neighboring glomeruli independent of their odorant receptor identity. *Communications Biology* **2**, 14 (2019).

34 Saraiva, L. R. *et al.* Combinatorial effects of odorants on mouse behavior. *Proceedings of the National Academy of Sciences* **113**, E3300-E3306 (2016).

35 Qiu, Q., Wu, Y., Ma, L. & Yu, C. R. Encoding Innately Recognized Odors via a Generalized Population Code. *bioRxiv*, 2020.2001.2028.923748 (2020).

36 Iurilli, G. & Datta, S. R. Population Coding in an Innately Relevant Olfactory Area. *Neuron* **93**, 1180-1197.e1187 (2017).

37 Bozza, T., McGann, J. P., Mombaerts, P. & Wachowiak, M. In vivo imaging of neuronal activity by targeted expression of a genetically encoded probe in the mouse. *Neuron* **42**, 9-21 (2004).

38 Ma, L. *et al.* Distributed representation of chemical features and tunotopic organization of glomeruli in the mouse olfactory bulb. *Proc Natl Acad Sci U S A* **109**, 5481-5486 (2012).

39 Franklin, K. B. & Paxinos, G. *The mouse brain in stereotaxic coordinates*. Vol. 3 (Academic press New York:, 2008).

40 Paxinos, G. & Franklin, K. (Academic Press: San Diego, 2013).

Figures

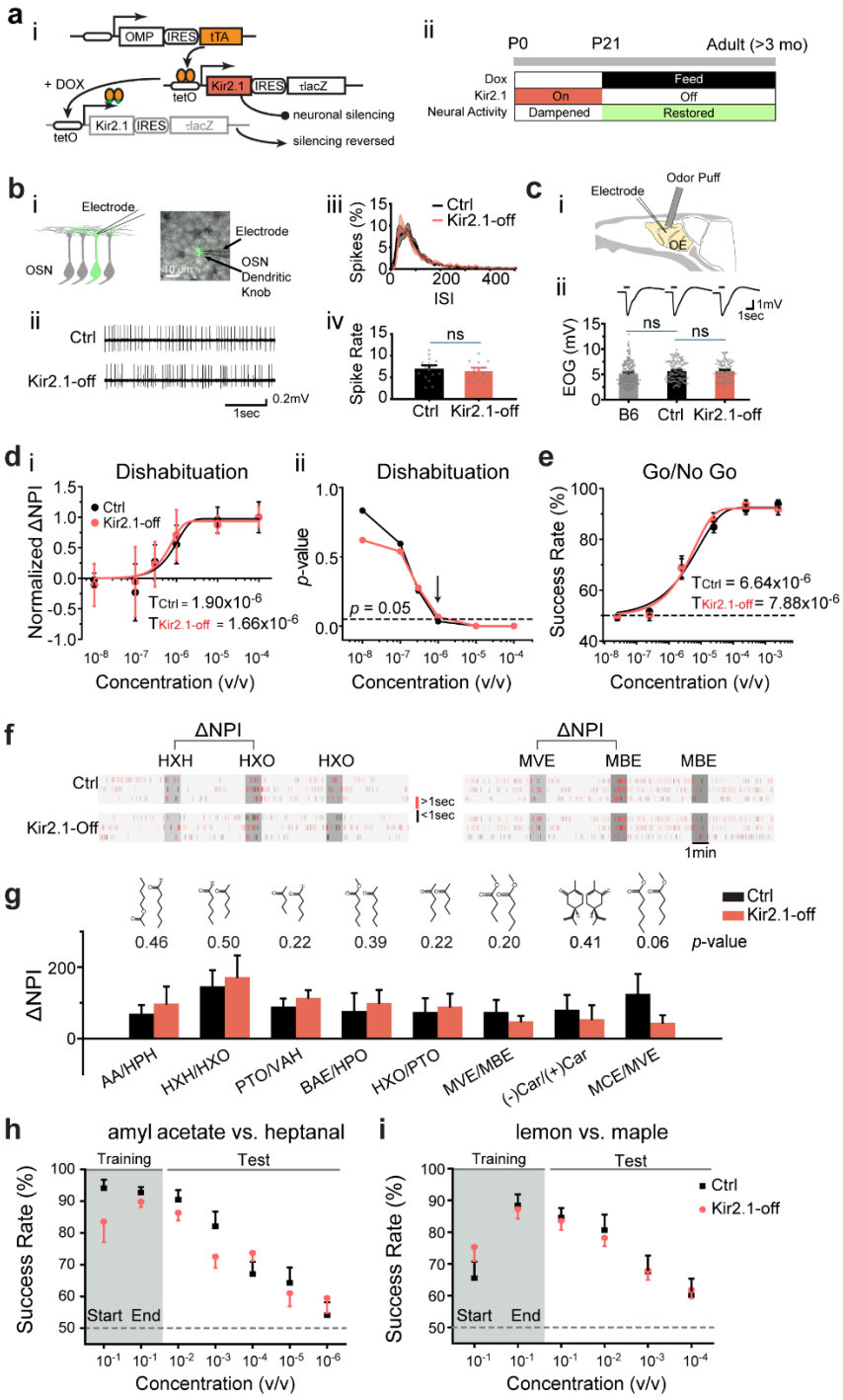
a
i
OMP
IRES
tTA
+ DOX
tetO
Kir2.1
IRES
τlacZ
neuronal silencing
silencing reversed
ii
P0
P21
Adult (>3 mo)
Dox
Feed
Kir2.1
On
Off
Neural Activity
Dampened
Restored
b
i
Electrode
OSN
Electrode
OSN
Dendritic
Knob
ii
Ctrl
Kir2.1-off
0.2mV
1sec
iii
Spikes (%)
Ctrl
Kir2.1-off
ISI
iv
Spike Rate
ns
Ctrl
Kir2.1-off
c
i
Electrode
Odor Puff
OE
ii
1mV
1sec
EOG (mV)
ns
ns
B6
Ctrl
Kir2.1-off
d
i
Dishabituation
Normalized ΔNPI
Ctrl
Kir2.1-off
TCtrl = 1.90x10-6
TKir2.1-off = 1.66x10-6
Concentration (v/v)
ii
Dishabituation
p-value
p = 0.05
Concentration (v/v)
e
Go/No Go
Success Rate (%)
TCtrl = 6.64x10-6
TKir2.1-off = 7.88x10-6
Concentration (v/v)
f
ΔNPI
HXH
HXO
HXO
MVE
MBE
MBE
Ctrl
Kir2.1-Off
>1sec
<1sec
1min
g
Ctrl
Kir2.1-off
0.46
0.50
0.22
0.39
0.22
0.20
0.41
0.06
p-value
ΔNPI
AA/HPH
HXH/HXO
PTO/VAH
BAE/HPO
HXO/PTO
MVE/MBE
(-)Car/(+)Car
MCE/MVE
h
amyl acetate vs. heptanal
Training
Test
Success Rate (%)
Start
End
Concentration (v/v)
i
lemon vs. maple
Training
Test
Ctrl
Kir2.1-off
Success Rate (%)
Start
End
Concentration (v/v)

Fig. 1: Suppressing spontaneous activity during early development does not impact odor detection, discrimination and association

a i. Illustration of the inducible transgene expression in the OMP-IRES-tTA/tetO-Kir2.1-IRES-tauLacZ mice. ii. Schematic illustration of genetic silencing OSNs during early postnatal period.

b i. Dendritic recording of an OSN in M72-GFP animal. Superimposed bright field and fluorescent images show a recording pipette attached to the dendritic knob of an M72-GFP OSN. ii. Raster plots showing examples of spontaneous spiking patterns of OSNs from control and Kir2.1-off mice. iii. Distribution of inter-spike interval (ISI) in control (black) and Kir2.1-off (red) animals. iv. Bar plot of average firing frequencies of M72 OSNs in control (black) and Kir2.1-off (red) mice.

c i. Illustration of electro-olfactogram (EOG) recording. ii. Response sample traces (top) and average amplitude (bottom) of C57Bl/6 (B6), littermate control (Ctrl) and Kir2.1-off mice.

d Detection threshold of amyl acetate is determined by dishabituation assay. i. Mean ΔNPI values for amyl acetate presented at different concentrations (10^{-8} to 10^{-4} v/v) for control (black) and Kir2.1-off (red) mice. Data are fitted with Weibull psychometric function with threshold values (T) shown. ii. *p*-values of ΔNPI at different odor concentrations from (i). Arrow indicates the concentration at which *p*-value is at 0.05. Dashed line indicates where the *p*-value is 0.05.

e Success rates in Go/No Go test with increasing odor concentrations of amyl acetate. Data are fitted with a Weibull psychometric function. Threshold values (T) calculated from the fitting are indicated. Dashed line in indicates success rate at chance level of 50%.

f Cross habituation test. Raster plots of odor port investigation by control (Ctrl) and Kir2.1-off mice. Animals are habituated with hexanal (HXH, left) or methyl valerate (MVE, right) before exposed to 2-hexanone (HXO, left) or methyl butyrate (MBE, right) respectively. Odor deliveries are marked by gray boxes. Only the last habituation and first two novel stimulation periods are shown.

g Bar plot of ΔNPI (mean ± SEM) in Ctrl (black) and Kir2.1-off (red) for discrimination of different odor pairs. Chemical structures of the odorants are shown. Numbers above the bars indicate the *p*-values between the scores obtained from Ctrl and Kir2.1-off.

h, i Two-choice odor discrimination assay. Scatter plots show the success rate for Ctrl (black) and Kir2.1-off (red) mice in discriminating amyl acetate versus heptanal (**h**), and lemon versus maple (**i**) at decreasing concentrations.

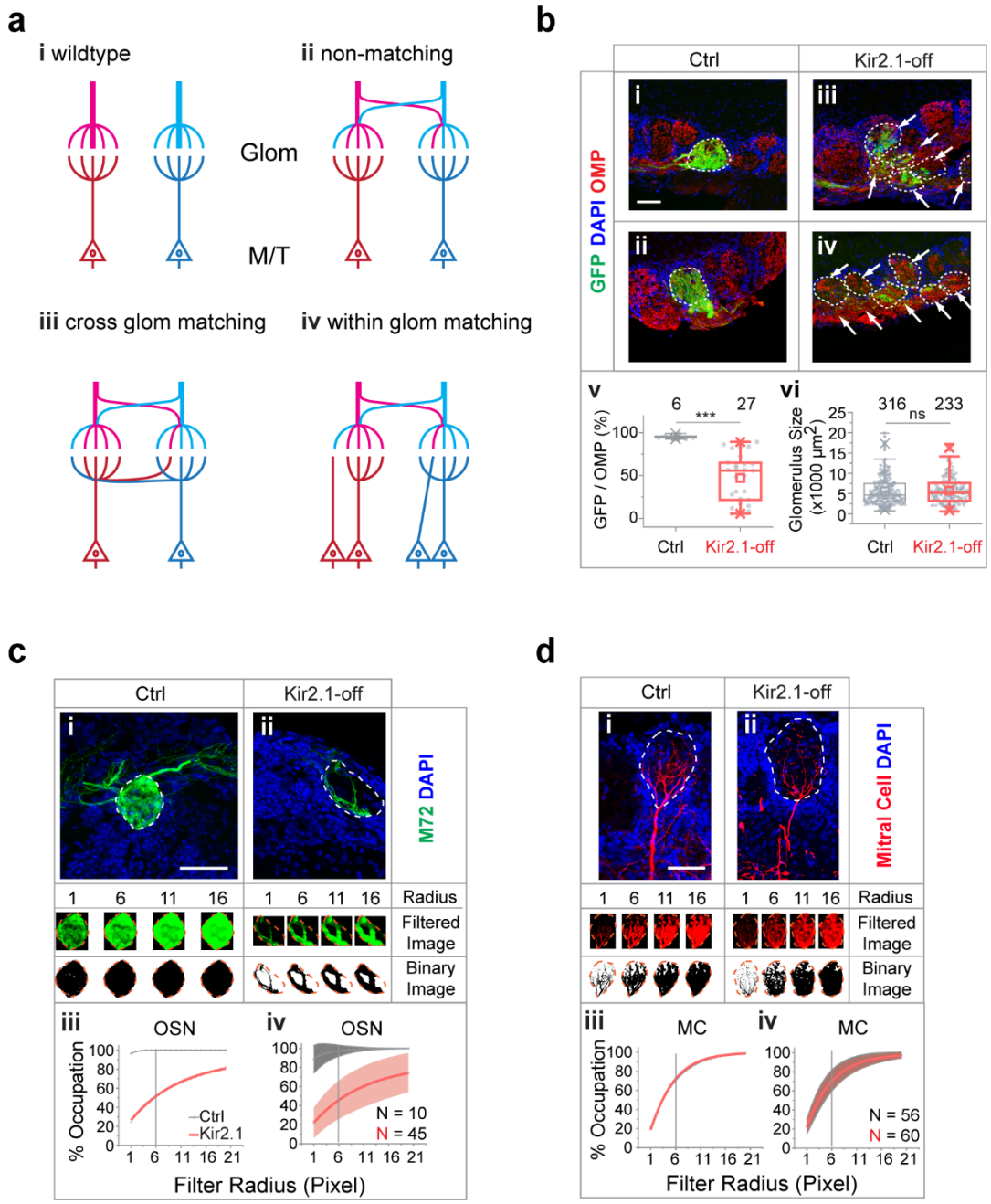

Fig. 2: Mismatch between OSN axons and M/T cell dendrites in Kir2.1-off mice.

a Models of connectivity between OSN axons and mitral/tufted cell dendrites. i, In the wildtype, each glomerulus receives input from axons expressing the same odorant

receptors (color coded), which are connected to the same primary dendrites of the mitral/tufted cells. ii, Divergent projection of OSN axons does not influence dendritic innervation such that the primary dendrites receive input from OSNs expressing different odorant receptors. iii, Axon-dendritic connection is made through cross-glomerular matching such that the same dendrite is always innervated by OSNs expressing the same odorant receptor. iv, Matching axon-dendritic connection is restricted only in the glomeruli.

b Confocal images of olfactory bulb sections from mice carrying homozygotic *M72-IRES-tauGFP* allele. Immunofluorescent signals show GFP (green), DAPI (blue) and OMP (red) in control (i and ii) and Kir2.1-off (iii and iv) mice. Dotted circles circumscribe the glomeruli containing green fibers. Glomeruli are identified based on the density of periglomerular cell nuclei. Arrows point to fibers in the glomerular layer that are not counted towards quantification. Scale bar, 50 µm. v. Quantification of the overlap between OMP signals and GFP signal in individual glomeruli in the control and Kir2.1-off mice. vi. Quantification of the glomerular size (diameter) in control and Kir2.1-off mice (N = 3 animals each). Numbers in the panel indicate the total glomeruli counted.

c Glomerular occupancy by OSN axons. Immunofluorescent staining in Ctrl (i) and Kir2.1-off (ii) mice to label *M72-IRES-GFP* axons (green). Spatial filters with 1-, 6-, 11-, 16-pixel radii were applied to obtain filtered images. After applying a binary threshold, any pixel that contains fluorescent signal is shown in black. Scale bar, 50 µm. Percentages of glomerular occupancy calculated as a function of filter radius are plotted for individual images (iii) for images shown in (i) and for all data (iv). Data are shown in mean (dashed line) ± standard deviation (shaded area).

d same as **c** but for mitral cell dendrites (BDA, red). Note that black and red lines almost overlap in iii and iv. Scale bar, 50 µm.

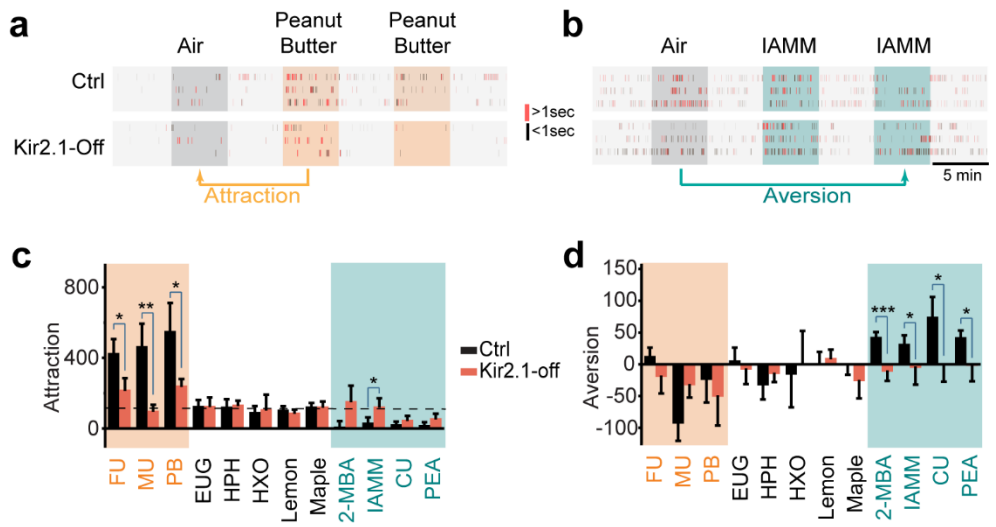

Fig. 3: Suppressing spontaneous activity during early development alters odor preference in adulthood.

a, b Raster plots of odor port investigation of air, peanut butter (**a**) and isoamylamine (IAMM, **b**). Each tick represents an investigation event. Investigations longer or shorter than 1 second are marked by red and black ticks, respectively.

c, d Bar graphs showing attraction (**c**) and aversion (**d**) indices for control (black) and Kir2.1-off (red) mice. The following odorants were used. Neutral odors, eugenol (EUG), heptanal (HPH), 2- hexanone (HXO), lemon and maple; attractive odors, peanut butter (PB), female urine (FU) and male urine (MU); aversive odors, 2-MBA, IAMM, coyote urine (CU) and 2-phenylethylamine (PEA). All bar graph data are shown in mean ± SEM.

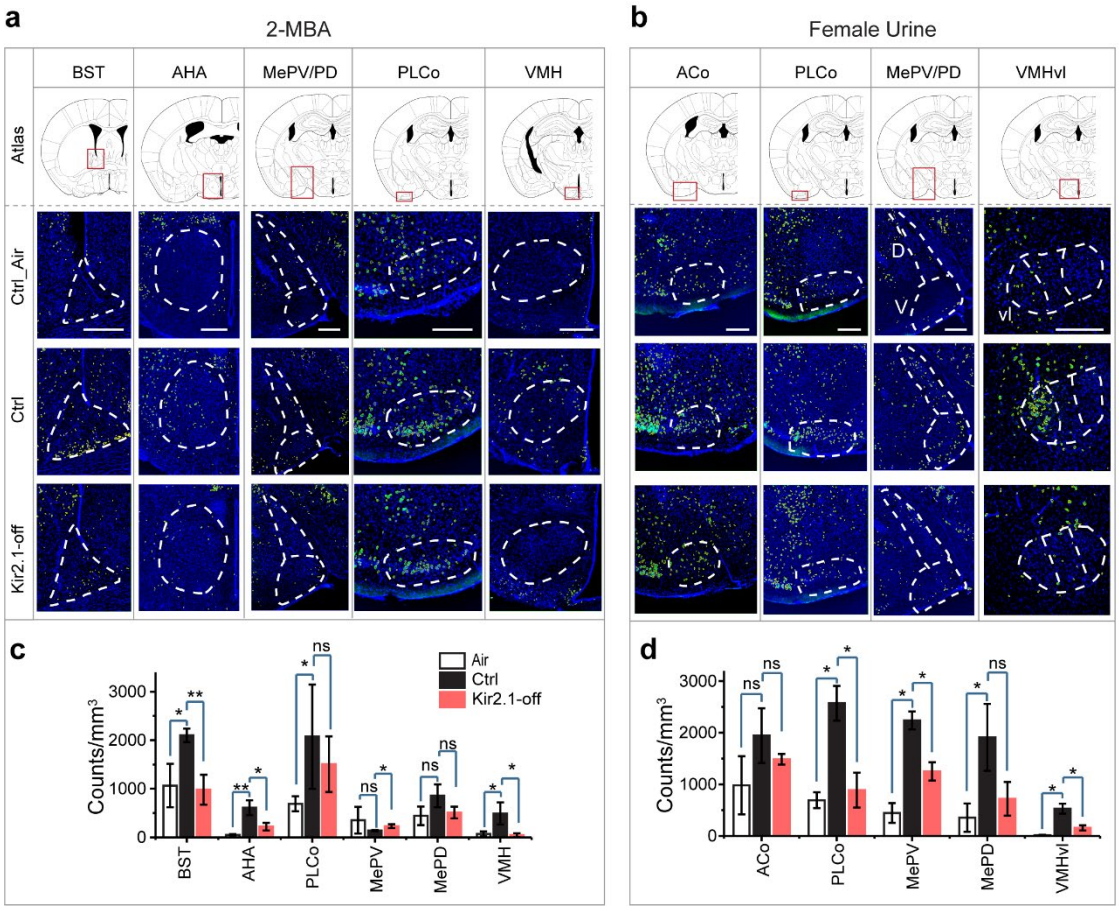

Fig. 4: Suppression of spontaneous activities during development alters representation of innate odors in the adult brain.

a, b Immunofluorescent staining of phospho-S6 (green) of brain sections from Ctrl and Kir2.1-off animals treated with 2-MBA (**a**) and female urine (**b**). Cell nuclei are counterstained with DAPI (blue). Top panel shows the atlas maps (adapted from The Mouse Brain Stereotaxic Coordinates) [40], with the boxes indicating the brain regions in the lower panels. Scale bar, 300 µm.

c, d Bar plots show the density of activated cells in different brain areas in Ctrl and Kir2.1-off mice (data are shown in mean ± SEM, n = 6 hemispheres). *, $p < 0.05$; **, $p < 0.01$; ***, $p < 0.01$; ns, not significant ($p > 0.05$).

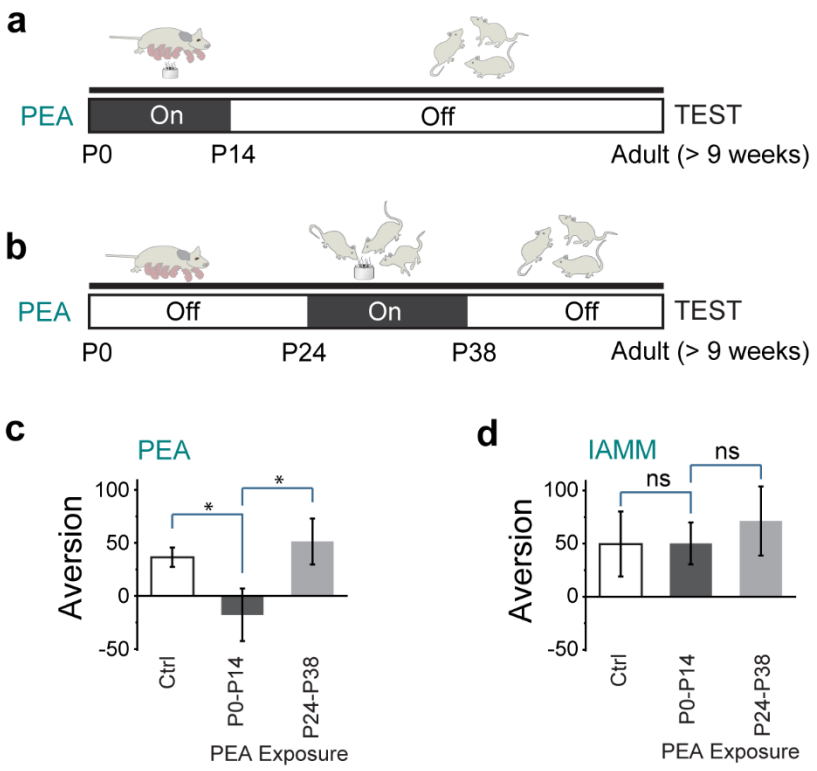

Fig. 5: Early postnatal exposure to aversive odor alters innate odor recognition in adulthood

a, b Schematic illustration of the experimental paradigms. Animals were raised and exposed to PEA between P0 and P14 (**a**) or between P24 and P38 (**b**). The animals were tested at adult stage.

c, d Bar plots of average aversion indices to PEA (**c**) and IAMM (**d**) in control (no exposure), P0 - P14 and P24 - P38 PEA exposed animals.

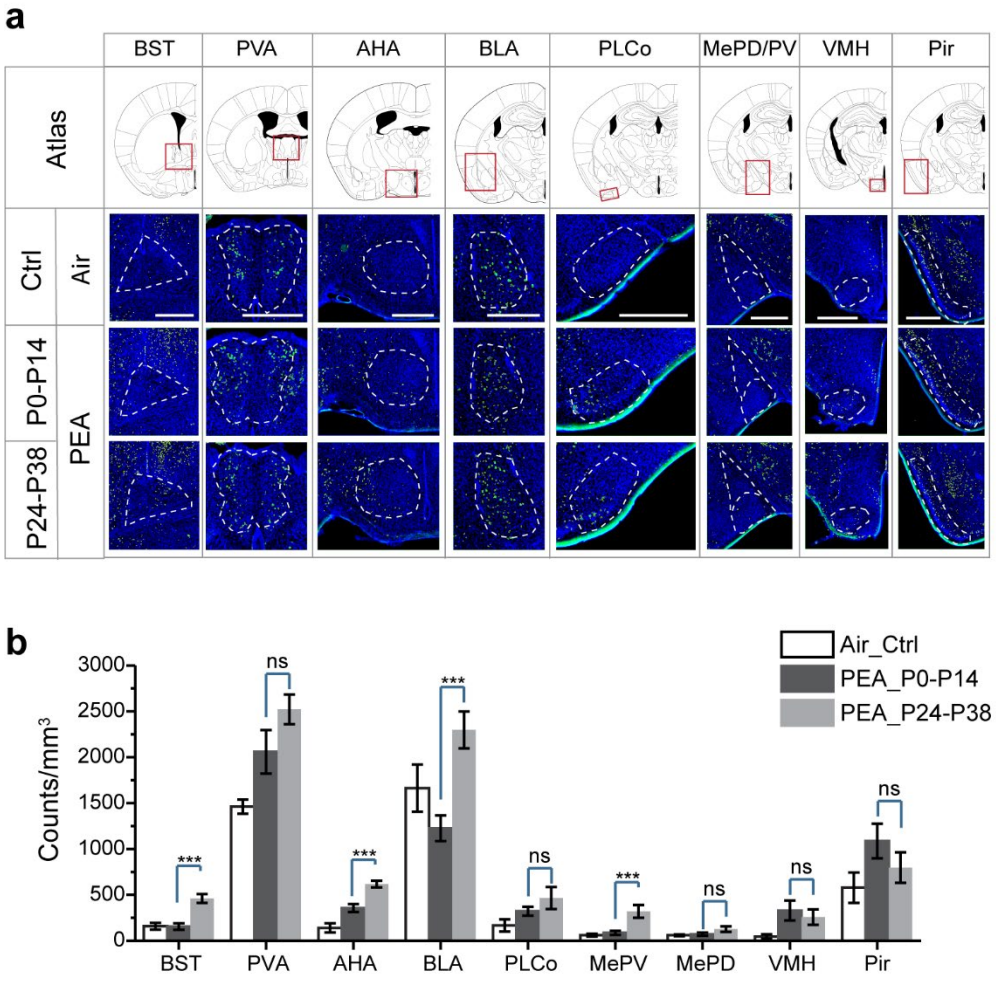

Fig. 6: Early postnatal exposure to aversive odor alters representation of innate odors in the adult brain.

a Immunofluorescent staining of phospho-S6 (green) of brain sections from PEA treated mice. Cell nuclei are counterstained with DAPI (blue). Scale bar, 500 µm.

b Bar plot shows the density of activated cells in different brain areas (data are shown in mean ± SEM, n = 6 hemispheres). Student *t*-test was applied. *, $p < 0.05$; **, $p < 0.01$; ***, $p < 0.01$; ns, not significant ($p > 0.05$).

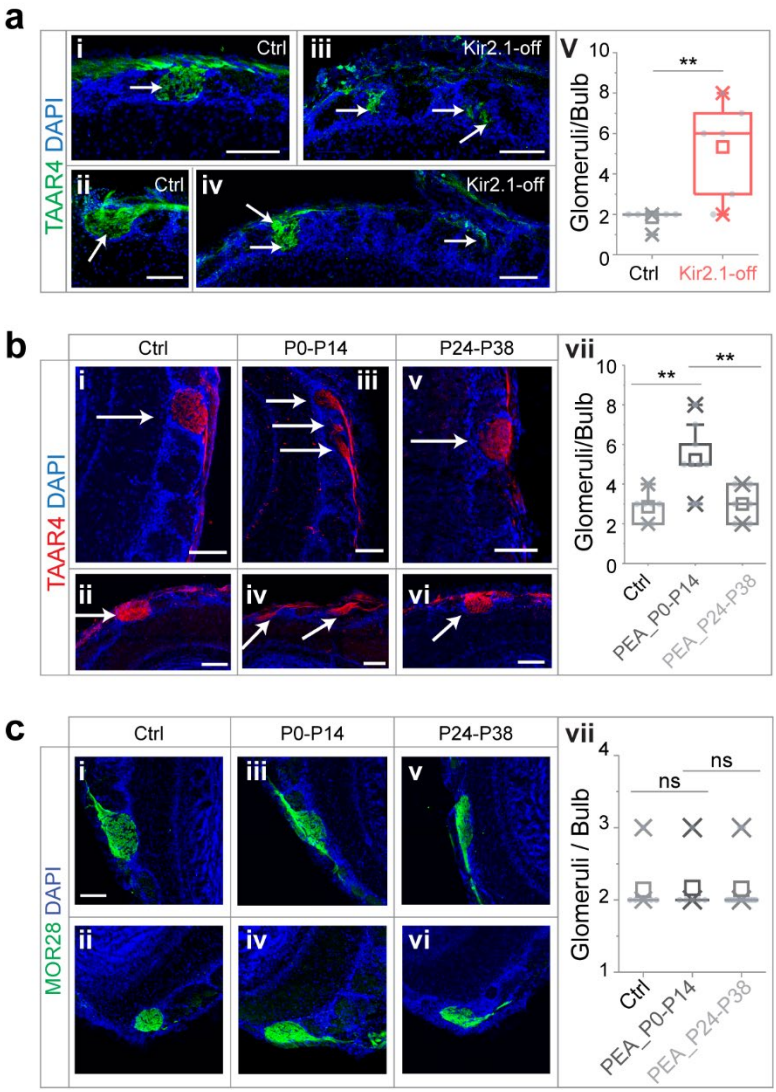

Fig. 7: Altered projection patterns of TAAR4 expressing OSN axons in Kir2.1-off and PEA treated mice.

a Immunofluorescent staining of TAAR4 receptor in olfactory bulb sections from control animals (i-ii) and Kir2.1-off animals (iii-iv). Green, TAAR4 signal. Blue, DAPI. v. Quantification of TAAR4^{+} glomeruli each OB. Box plot edges indicate the first and third quartiles of the data, while whiskers indicate 1.5 interquartile range.

b TAAR4 staining of olfactory bulb sections for control (i-ii), P0 - P14 PEA exposed (iii-iv) and P24 - P38 exposed (v-vi) animals. Red, TAAR4. Blue: DAPI. vii. Quantification of $TAAR4^{+}$ glomeruli for each OB.

c Confocal images of MOR28 receptor immunofluorescent staining in olfactory bulb sections for control (i-ii), P0 - P14 PEA exposed (iii-iv) and P24 - P38 exposed (v-vi) animals. Green, MOR28. Blue: DAPI. vii. Quantification of MOR28 + glomeruli for each OB. Student *t*-test result is shown. **, $p < 0.01$. Arrows point to each glomerulus. Scale bars, 100 µm.

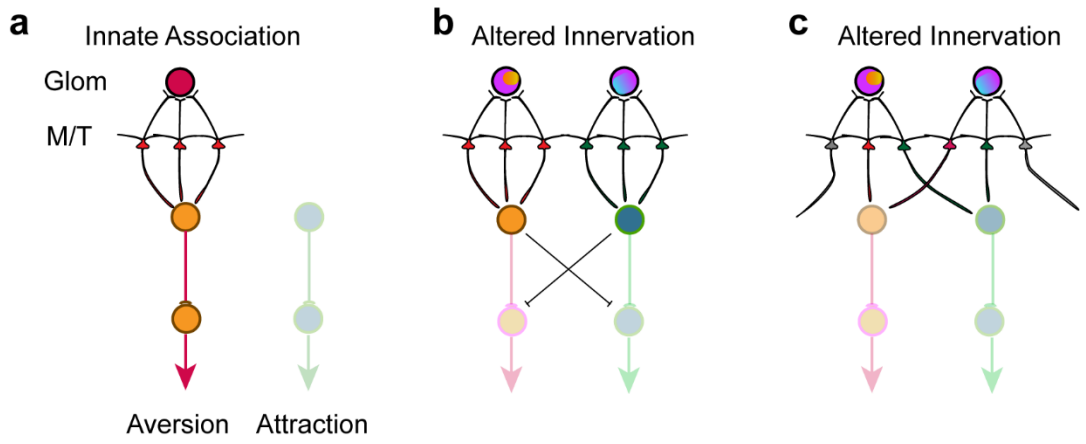

Fig. 8: Models of encoding innate valence of odors

a Wildtype connections model. The activation of specific glomeruli leads to the activation of specific sets of mitral/tufted cells that connect to behavioral centers.

b Altered axon innervation model. Activation pattern with altered axon projection leads to the activations of brain centers that drive opposing behaviors and abolished innate responses normally associated with the same odor.

c Alternative altered axon innervation model. The change of activity pattern of the mitral/tufted cells is not the result of direct relay from the glomerular activation but the result of intercell interactions within the olfactory bulb. This change removes the biased activation of appetitive or aversive responses to abolish innate preference.